that the expression level of H-FABP was significantly different between the responder (PR and CR) and nonresponder (PD) groups (P = 0.0031, Mann-Whitney U test) and also between the patients with MR or SD and the nonresponder group (P = 0.0047, Mann-Whitney U test). These results indicate that up-regulation of H-FABP in tumor tissues can be monitored by routine clinical methods.

Discussion

We identified 87 protein spots of which the intensity was statistically significantly different between samples from the responder (CR and PR) and nonresponder (PD) groups in the training set. Application of a data-mining procedure allowed identification of a set of nine protein spots that accurately distinguished between responders and nonresponders. The different expression levels of these nine protein spots allowed classification of 13 of 14 of our test PR and PD cases in accordance with their clinical response to gefitinib. These protein spots classified cases showing a MR to gefitinib (MR) into the responder group. The intermediate cases, SD, were categorized into both responder and nonresponder groups. The usefulness of our findings will be validated in a larger clinical data set.

Table 3. List of proteins for the response to gefitinib

Spots no.*	Rank	Accession no.†	Identtified protein†	MW (DA)‡	pI‡	Ion charge state (+)	MZ (obs)§	Mass‖	δ¶	Miss**	Mascot ions score††	Peptide sequence
384	5	Q96RP9	Ig mu chain C region	49,557	6.35	2	810.3	1,617.7	0.91	0	74	QVGSGVTTDQVQAEAK
						2	640.1	1,277.5	0.63	0	47	YAATSQVLLPSK
671	1	P01876	Ig α-1 chain C region	37,655	6.08	2	919.2	1,836.0	0.32	0	68	QEPSQGTTTFAVTSILR
						2	771.8	1,540.7	0.91	0	54	DASGVTFTWTPSSGK
1090	7	Q9UNH7	SNX 6	46,649	5.81	2	636.5	1,270.5	0.55	0	73	NLVELAELELK
						2	577.0	1,152.2	−0.33	0	39	SLVDYENANK
1182	8	P50453	Cytoplasmic antiproteinase 3	42,404	5.61	2	816.4	1,629.8	0.95	0	82	IEELLPGSSIDAETR
						2	626.6	1,249.4	1.66	0	75	AFQSLLTEVNK
						2	591.0	1,179.5	0.47	0	63	LVLVNAIYFK
						2	757.5	1,513.6	−0.56	0	47	LQEDYDMESVLR +Oxidation (M)
1292	6	P40121	Macrophage capping protein	38,518	5.88	2	633.8	1,264.4	1.18	0	85	VSDATGQMNLTK
						2	676.8	1,351.4	0.05	0	79	YQEGGVESAFHK
						2	932.1	1,861.1	1.11	0	50	MQYAPNTQVEILPQGR +Oxidation (M)
						2	659.8	1,317.3	0.23	0	41	EGNPEEDLTADK
1711	3	Q8NBJ7	Sulfatase modifying factor 2	33,857	7.78	2	792.5	1,581.7	1.32	0	112	MGNTPDSASDNLGFR
						2	779.9	1,557.6	0.15	0	95	GASWIDTADGSANHR
						2	740.0	1,477.6	0.36	0	83	LPTEEEWEFAAR
						2	613.2	1,224.4	−0.02	0	66	FLMGTNSPDSR
						2	629.9	1,256.5	1.27	0	55	SVLWWLPVEK
						2	818.0	1,633.8	0.12	1	55	RLPTEEEWEFAAR
						2	837.7	1,672.9	0.48	0	47	LEHPVLHVSWNDAR
2091	9	P09211	Glutathione *S*-transferase P	23,225	5.44	2	647.5	1,292.5	0.44	0	36	MLLADQGQSWK +Oxidation (M)
2182	4	P02794	Ferritin heavy chain	21,094	5.30	2	823.4	1,643.8	1.04	0	91	MGAPESGLAEYLFDK +Oxidation (M)
						2	648.3	1,294.5	0.03	0	53	NVNQSLLELHK
2478	2	P05413	Fatty acid-binding protein, heart	14,727	6.34	2	735.2	1,467.5	0.81	0	103	LGVEFDETTADDR
						2	798.7	1,595.7	−0.32	1	73	LGVEFDETTADDRK
						2	603.3	1,204.3	0.26	0	70	WDGQETTLVR
						2	455.0	907.0	1.04	0	67	SLGVGFATR
						2	774.7	1,546.8	0.56	0	61	QVASMTKPTTIIEK
						2	438.0	873.0	0.88	0	54	NGDILTLK
						1	889.6	889.0	−0.41	0	45	SIVTLDGGK

Abbreviation: pI, isoelectric point.
*Spot numbers refer to those in Fig. 1B (Supplementary Fig. S3).
†Accession nos. of proteins were derived from Swiss-Prot and National Center for Biotechnology Information nonredundant databases.
‡Theoretical molecular weight and isoelectric point were obtained from Swiss-Prot and the ExPASy database (http://au.expasy.org).
§Experimental m/z value.
‖Relative molecular mass calculated from the peptide sequence.
¶Difference (error) between the experimental and calculated masses.
**Number of missed cleavage sites.
††Mascot ions score (http://www.matrixscience.com/search_form_select.html).

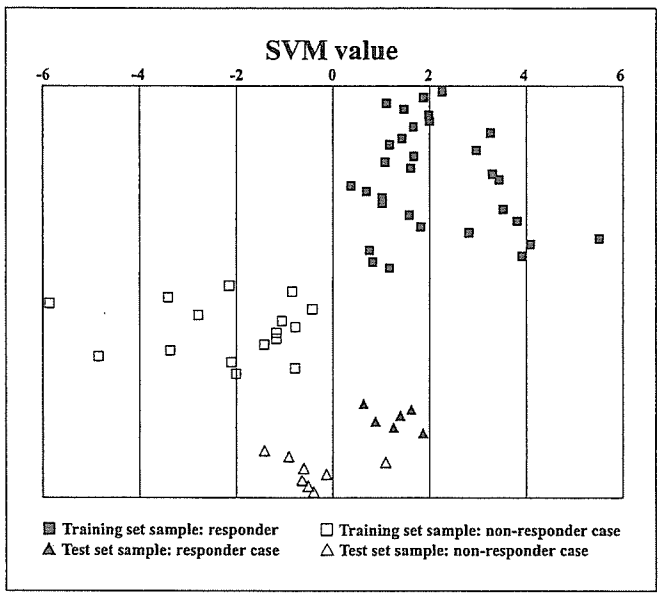

Fig. 2. Predictive performance of the nine spots was validated by examining the SVM value of each sample in the group.

We identified the proteins whose expression was correlated with response to gefitinib and found associations with the EGFR signal pathway and with the biology of lung cancer. Sorting nexin (SNX) 6 is a member of a SNX family that functions in the intracellular trafficking of plasma membrane receptors (33). SNXs form complexes with other SNXs and with plasma membrane receptors. In complexes with SNX1, SNX2, and SNX4, SNX6 interacts with the intercellular portion of the EGFR as well as with transforming growth factor-β receptor, insulin receptor, leptin receptor, and platelet-derived growth factor receptor (34). By binding to the kinase domain of the transforming growth factor-β receptor, SNX6 perturbs transforming growth factor-β signal transduction (34). The other SNX family, SNX1, decreases the expression of EGFR by activating the endosome-to-lysosome pathway with enterophilin-1 (35), although the functions of the complex of SNX6 and EGFR have not yet been reported. The functional association of SNX6 with oncogene product Pim-1, which has been implicated in the development of hematopoietic (36), gastric (37), and prostatic (38) malignancies, suggests the involvement of SNX6 in cancer biology. Kakiuchi et al. (21) reported that another SNX family member, SNX13, was correlated with the response to gefitinib in patients with NSCLC. These reports suggest that SNX6 might play an important role in signal transduction pathways that affect the phenotypes of lung cancer.

We tried to identify the proteins whose expression was associated with EGFR mutation. Because gefitinib is a specific inhibitor of EGFR and mutation of EGFR is considered to be a predictive marker for gefitinib sensitivity, we had expected some similarity between the set of proteins predicting sensitivity to gefitinib and the set of proteins reflecting EGFR mutation status. However, only sulfate modifying factor 2 was common to the two sets. Search of the PubMed database revealed no association of sulfate modifying factor 2 with the EGFR pathway and no evidence for its involvement in resistance to chemotherapy. Similarly, the other proteins correlated with EGFR mutation status had no obvious involvement in the EGFR pathway. Functional studies on these proteins will contribute to further understanding of EGF signaling in cells and to discovery of novel therapeutic targets in lung cancer.

2D-DIGE is a high-performance proteomic technology and a powerful tool to develop candidate biomarkers. However, 2D-DIGE requires expensive fluorescent dyes and well-trained operators to run the gels. Thus, routine clinical studies with multiple large-format two-dimensional gels and a 2D-DIGE protocol are unlikely to be practical. Application of our results requires a simple and cost-effective method that can be used routinely in the clinic. In addition, as we need to examine the expression of multiple proteins, a practical tool for simultaneously measuring the amount of the other proteins is required. With that in mind, we validated measurement of the differential expression of H-FABP by the use of a commercially available ELISA kit (MARLIT-M H-FABP) that is routinely used in hospitals for the early diagnosis of acute myocardial infarction using serum samples. The expression level of H-FABP in tumor tissues as monitored by the ELISA assay was highly correlated with that by 2D-DIGE, and a significant difference in H-FABP expression was observed between responders (CR + PR), minor responders (MR + SD), and nonresponders (PD). Thus, our results can provide a simple and direct method to predict the response to gefitinib.

H-FABP functions in intracellular lipid transport, storage, and metabolism. As H-FABP is highly expressed in heart and released into plasma after myocardial injury, it has been used as a plasma marker for early diagnosis of acute myocardial infarction and stroke. However, many lines of evidence also suggest an association of H-FABP with cancer biology. Higher expression of H-FABP was observed in a more tumorigenic small-cell lung cancer cell line (39) compared with its counterpart. Increased expression of H-FABP is associated with tumor aggressiveness, metastasis, and poor prognosis of gastric cancer (40). In contrast, H-FABP is known to have growth-inhibitory activity in breast cancer cells (41), and breast cancer does not express H-FABP because of gene silencing by hypermethylation (42). These observations suggest complexity in the way that H-FABP is involved in the progression of cancer. Recently, Loeffler-Ragg et al. (43) reported that another FABP family member, E-FABP, is up-regulated in gefitinib-resistant colon cancer cell lines compared with gefitinib-sensitive cell

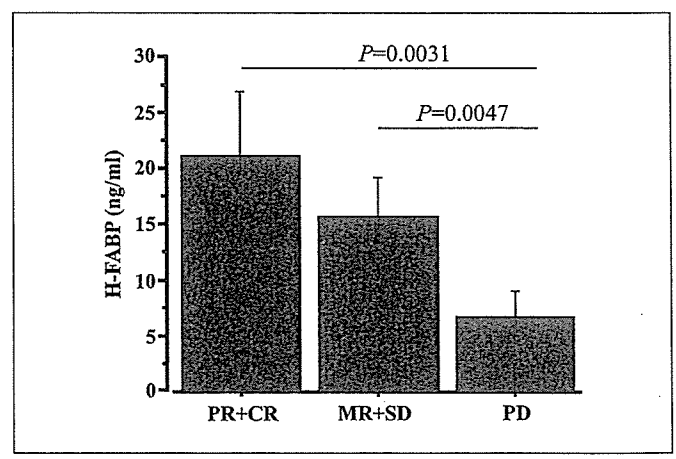

Fig. 3. ELISA assay for H-FABP. The differential expression level of H-FABP was validated by ELISA assay.

lines. Further study on the contribution of the FABP family to cancer phenotypes, including resistance to chemotherapy, will provide novel insights into cancer biology.

In conclusion, our proteomic study has identified proteins whose expression can predict the response to gefitinib in patients with recurrence of lung adenocarcinoma. Large-scale validation of the present results and functional analysis to elucidate the contribution and synergies of the identified proteins in the response to gefitinib will assist in developing novel therapeutic strategies for lung cancer.

References

1. Breathnach OS, Freidlin B, Conley B, et al. Twenty-two years of phase III trials for patients with advanced non-small-cell lung cancer: sobering results. J Clin Oncol 2001;19:1734–42.
2. Herbst RS. Dose-comparative monotherapy trials of ZD1839 in previously treated non-small cell lung cancer patients. Semin Oncol 2003;30:30–8.
3. Fukuoka M, Yano S, Giaccone G, et al. Multi-institutional randomized phase II trial of gefitinib for previously treated patients with advanced non-small-cell lung cancer (The IDEAL 1 Trial). J Clin Oncol 2003; 21:2237–46.
4. Kris MG, Natale RB, Herbst RS, et al. Efficacy of gefitinib, an inhibitor of the epidermal growth factor receptor tyrosine kinase, in symptomatic patients with non-small cell lung cancer: a randomized trial. JAMA 2003;290:2149–58.
5. Inoue A, Saijo Y, Maemondo M, et al. Severe acute interstitial pneumonia and gefitinib. Lancet 2003;361: 137–9.
6. Takano T, Ohe Y, Kusumoto M, et al. Risk factors for interstitial lung disease and predictive factors for tumor response in patients with advanced non-small cell lung cancer treated with gefitinib. Lung Cancer 2004;45:93–104.
7. Miller VA, Kris MG, Shah N, et al. Bronchioloalveolar pathologic subtype and smoking history predict sensitivity to gefitinib in advanced non-small-cell lung cancer. J Clin Oncol 2004;22:1103–9.
8. Takano T, Ohe Y, Sakamoto H, et al. Epidermal growth factor receptor gene mutations and increased copy numbers predict gefitinib sensitivity in patients with recurrent non-small-cell lung cancer. J Clin Oncol 2005;23:6829–37.
9. Paez JG, Janne PA, Lee JC, et al. EGFR mutations in lung cancer: correlation with clinical response to gefitinib therapy. Science 2004;304:1497–500.
10. Lynch TJ, Bell DW, Sordella R, et al. Activating mutations in the epidermal growth factor receptor underlying responsiveness of non-small-cell lung cancer to gefitinib. N Engl J Med 2004;350:2129–39.
11. Cappuzzo F, Gregorc V, Rossi E, et al. Gefitinib in pretreated non-small-cell lung cancer (NSCLC): analysis of efficacy and correlation with HER2 and epidermal growth factor receptor expression in locally advanced or metastatic NSCLC. J Clin Oncol 2003; 21:2658–63.
12. Pao W, Miller VA. Epidermal growth factor receptor mutations, small-molecule kinase inhibitors, and non-small-cell lung cancer: current knowledge and future directions. J Clin Oncol 2005;23:2556–68.
13. Baselga J, Rischin D, Ranson M, et al. Phase I safety, pharmacokinetic, and pharmacodynamic trial of ZD1839, a selective oral epidermal growth factor receptor tyrosine kinase inhibitor, in patients with five selected solid tumor types. J Clin Oncol 2002;20: 4292–302.
14. Moasser MM, Basso A, Averbuch SD, Rosen N. The tyrosine kinase inhibitor ZD1839 ("Iressa") inhibits HER2-driven signaling and suppresses the growth of HER2-overexpressing tumor cells. Cancer Res 2001; 61:7184–8.
15. Janmaat ML, Kruyt FA, Rodriguez JA, Giaccone G. Response to epidermal growth factor receptor inhibitors in non-small cell lung cancer cells: limited antiproliferative effects and absence of apoptosis associated with persistent activity of extracellular signal-regulated kinase or Akt kinase pathways. Clin Cancer Res 2003; 9:2316–26.
16. Cappuzzo F, Hirsch FR, Rossi E, et al. Epidermal growth factor receptor gene and protein and gefitinib sensitivity in non-small-cell lung cancer. J Natl Cancer Inst 2005;97:643–55.
17. Hirsch FR, Varella-Garcia M, Bunn PA, Jr., et al. Epidermal growth factor receptor in non-small-cell lung carcinomas: correlation between gene copy number and protein expression and impact on prognosis. J Clin Oncol 2003;21:3798–807.
18. Hirata A, Hosoi F, Miyagawa M, et al. HER2 overexpression increases sensitivity to gefitinib, an epidermal growth factor receptor tyrosine kinase inhibitor, through inhibition of HER2/HER3 heterodimer formation in lung cancer cells. Cancer Res 2005;65:4253–60.
19. Cappuzzo F, Magrini E, Ceresoli GL, et al. Akt phosphorylation and gefitinib efficacy in patients with advanced non-small-cell lung cancer. J Natl Cancer Inst 2004;96:1133–41.
20. Han SW, Hwang PG, Chung DH, et al. Epidermal growth factor receptor (EGFR) downstream molecules as response predictive markers for gefitinib (Iressa, ZD1839) in chemotherapy-resistant non-small cell lung cancer. Int J Cancer 2005;113:109–15.
21. Kakiuchi S, Daigo Y, Ishikawa N, et al. Prediction of sensitivity of advanced non-small cell lung cancers to gefitinib (Iressa, ZD1839). Hum Mol Genet 2004;13: 3029–43.
22. Zembutsu H, Ohnishi Y, Daigo Y, et al. Gene-expression profiles of human tumor xenografts in nude mice treated orally with the EGFR tyrosine kinase inhibitor ZD1839. Int J Oncol 2003;23:29–39.
23. Jain A, Tindell CA, Laux I, et al. Epithelial membrane protein-1 is a biomarker of gefitinib resistance. Proc Natl Acad Sci U S A 2005;102:11858–63.
24. Gygi SP, Rochon Y, Franza BR, Aebersold R. Correlation between protein and mRNA abundance in yeast. Mol Cell Biol 1999;19:1720–30.
25. Chen G, Gharib TG, Wang H, et al. Protein profiles associated with survival in lung adenocarcinoma. Proc Natl Acad Sci U S A 2003;100:13537–42.
26. Travis WD, Colby TV, Corrin B, Shimosato Y, Brambilla E. Histological typing of lung and pleural tumours. World Health Organization International Classification of Tumors. New York (NY): Springer-Verlag; 1999.
27. Colby TV, Noguchi M, Henschke C, et al. Adenocarcinoma. In: Travis WD, Brambilla E, Muller-Hermelink HK, Harris CC, editors. Pathology and genetics: tumors of the lung, pleura, thymus, and heart. Lyon (France): IARC; 2004. p. 35–44.
28. Ebright MI, Zakowski MF, Martin J, et al. Clinical pattern and pathologic stage but not histologic features predict outcome for bronchioloalveolar carcinoma. Ann Thorac Surg 2002;74:1640–6.
29. Green S, Weiss GR. Southwest Oncology Group standard response criteria, endpoint definitions and toxicity criteria. Invest New Drugs 1992;10:239–53.
30. Fujii K, Kondo T, Yokoo H, Yamada T, Iwatsuki K, Hirohashi S. Proteomic study of human hepatocellular carcinoma using two-dimensional difference gel electrophoresis with saturation cysteine dye. Proteomics 2005;5:1411–22.
31. Alban A, David SO, Bjorkesten L, et al. A novel experimental design for comparative two-dimensional gel analysis: two-dimensional difference gel electrophoresis incorporating a pooled internal standard. Proteomics 2003;3:36–44.
32. Brown MP, Grundy WN, Lin D, et al. Knowledge-based analysis of microarray gene expression data by using support vector machines. Proc Natl Acad Sci U S A 2000;97:262–7.
33. Worby CA, Dixon JE. Sorting out the cellular functions of sorting nexins. Nat Rev Mol Cell Biol 2002;3: 919–31.
34. Parks WT, Frank DB, Huff C, et al. Sorting nexin 6, a novel SNX, interacts with the transforming growth factor-β family of receptor serine-threonine kinases. J Biol Chem 2001;276:19332–9.
35. Pons V, Peres C, Teulie JM, et al. Enterophilin-1 interacts with focal adhesion kinase and decreases β1 integrins in intestinal Caco-2 cells. J Biol Chem 2004;279:9270–7.
36. Hammerman PS, Fox CJ, Birnbaum MJ, Thompson CB. Pim and Akt oncogenes are independent regulators of hematopoietic cell growth and survival. Blood 2005;105:4477–83.
37. Chen CN, Lin JJ, Chen JJ, et al. Gene expression profile predicts patient survival of gastric cancer after surgical resection. J Clin Oncol 2005;23: 7286–95.
38. Xie Y, Xu K, Dai B, et al. The 44 kDa Pim-1 kinase directly interacts with tyrosine kinase Etk/BMX and protects human prostate cancer cells from apoptosis induced by chemotherapeutic drugs. Oncogene 2006;25:70–8.
39. Zhang L, Cilley RE, Chinoy MR. Suppression subtractive hybridization to identify gene expressions in variant and classic small cell lung cancer cell lines. J Surg Res 2000;93:108–19.
40. Hashimoto T, Kusakabe T, Sugino T, et al. Expression of heart-type fatty acid-binding protein in human gastric carcinoma and its association with tumor aggressiveness, metastasis, and poor prognosis. Pathobiology 2004;71:267–73.
41. Huynh HT, Larsson C, Narod S, Pollak M. Tumor suppressor activity of the gene encoding mammary-derived growth inhibitor. Cancer Res 1995;55: 2225–31.
42. Huynh H, Alpert L, Pollak M. Silencing of the mammary-derived growth inhibitor (MDGI) gene in breast neoplasms is associated with epigenetic changes. Cancer Res 1996;56:4865–70.
43. Loeffler-Ragg J, Skvortsov S, Sarg B, et al. Gefitinib-responsive EGFR-positive colorectal cancers have different proteome profiles from non-responsive cell lines. Eur J Cancer 2005;41:2338–46.
44. Oken MM, Creech RH, Tormey DC, et al. Toxicity and response criteria of the Eastern Cooperative Oncology Group. Am J Clin Oncol 1982;5: 649–55.

 DOI 10.1002/pmic.200600196 *Proteomics* 2006, *6*, 4402–4409

RESEARCH ARTICLE

Proteomic signatures corresponding to histological classification and grading of soft-tissue sarcomas

Yoshiyuki Suehara[1, 2], Tadashi Kondo[1], Kiyonaga Fujii[3], Tadashi Hasegawa[4]**, Akira Kawai[5], Kunihiko Seki[4], Yasuo Beppu[5], Toshihide Nishimura[3], Hisashi Kurosawa[2] and Setsuo Hirohashi[1]*

[1] Proteome Bioinformatics Project, National Cancer Center Research Institute, Tokyo, Japan
[2] Department of Orthopedic Surgery, Juntendo University School of Medicine, Tokyo, Japan
[3] Clinical Proteome Center, Tokyo Medical University, Tokyo, Japan
[4] Pathology Division, National Cancer Center Research Institute, Tokyo, Japan
[5] Orthopedic Surgery Division, National Cancer Center Hospital, Tokyo, Japan

We performed a global protein expression study on soft-tissue sarcoma in order to develop novel diagnostic biomarkers and allow molecular classification. 2-D difference gel electrophoresis was used to generate the global protein expression profiles of 80 soft-tissue sarcoma samples with seven different histological backgrounds. We found that 67 protein spots distinguished the subtypes of soft-tissue sarcoma. Hierarchical clustering with these 67 protein spots resulted in the grouping of all 80 sarcoma samples corresponding to the histological classification. We found that the expression pattern of tropomyosin isoforms was different in conventional and pleomorphic leiomyosarcomas. We also identified five proteins, including alpha-1-antitrypsin, alpha-actinin 1, HSP27, and elongation factor 2, that could differentiate between malignant fibrous histiocytomas and leiomyosarcomas in grade III into low-risk and high-risk groups, which differed significantly with respect to survival. These results establish proteomics as a powerful tool to develop novel biomarkers for diagnosis and molecular classification of soft-tissue sarcomas. Identification of proteins associated with survival in grade III sarcoma will allow delineation of a high-risk group that may benefit from adjuvant therapy and the exclusion of low-risk patients in whom additional therapies are unlikely to exhibit clinical benefit.

Received: March 20, 2006
Accepted: May 11, 2006

Keywords:
2D-DIGE / Histological classification / Histological grading / Soft-tissue sarcoma / Toropomyosin

1 Introduction

Soft-tissue sarcoma is a rare malignant tumor. As the therapeutic response often depends on the histological subclass [1], accurate histological diagnosis is crucial to predict the biological behavior of the tumor and establish a therapeutic strategy. The subtypes of soft-tissue sarcoma are diagnosed by morphological findings, immunophenotyping, and karyotyping assisted by molecular analysis of specific-gene rearrangements. However, the wide range of histological appearance of soft-tissue tumors occasionally results in low validity and reproducibility of histological diagnosis and grading [2]. Molecular aberrations are not always consistent

Correspondence: Dr. Tadashi Kondo, Proteome Bioinformatics Project, National Cancer Center Research Institute, 5-1-1 Tsukiji, Chuo-ku, Tokyo 104-0045, Japan
E-mail: takondo@gan2.res.ncc.go.jp
Fax: +81-3-357-5298

Abbreviations: GIST, gastrointestinal stromal tumors; **MFH**, malignant fibrous histiocytomas

* Present address: Proteome Bioinformatics Project, National Cancer Center Research Institute, Tokyo, Japan
** Present address: Department of Clinical Pathology, Sapporo Medical University School of Medicine, Sapporo, Japan

in the same tumor type, and not all tumors have typical gene rearrangements [3]. Thus, novel approaches are needed to overcome some of the limitations of the present studies.

Recent development in cancer biology has been the study of global protein expression, an approach known as proteomics. DNA microarray technologies have also been applied at a genome-wide scale to the development of biomarkers for soft-tissue tumors, and several candidates have been identified [4–6]. However, RNA analysis alone cannot predict the functional features of the products such as PTMs, subcellular location, and association with ligands, as well as the rate of change with time of such properties, and these factors play important roles in the malignant behavior of tumor cells. Further, many lines of evidence have indicated discordance between mRNA expression and protein expression [7–9]. These difficulties underline the potential advantages of a proteomic rather than a transcriptomic approach. In addition, as the findings at the protein level will be more applicable to the subsequent immunohistochemical studies, the results can be validated using numerous paraffin-embedded tissues with clinical information by specific antibody. Proteomic technologies have been used to develop novel molecular subclassifications and diagnostic biomarkers for lung cancer [10, 11], ovarian tumors [12], breast cancer [13, 14], leukemia [15], and prostate cancer [9].

We performed a proteomic study of a panel of 80 soft-tissue sarcomas representing different histological subtypes and grading. We identified protein clusters that define histological subclasses and that differentiate low-risk from high-risk grade III groups, which differed significantly with respect to survival, of malignant fibrous histiocytomas (MFH) and leiomyosarcomas. This is the first systematic large-scale proteomic study to identify proteins associated with the histological subtypes and grading of soft-tissue sarcomas.

2 Materials and methods

The procedures that are only briefly described here are described in detail in Supplementary Text.

2.1 Patient population and protein extraction

We used tissue specimens from 80 soft-tissue sarcomas that had been surgically resected at the National Cancer Center Hospital in the period between 1996 and 2004. This project was approved by the Institutional Review Board of the National Cancer Center. The tumors comprised seven histological subgroups: 6 clear cell sarcomas, 10 myxoid liposarcomas, 9 gastrointestinal stromal tumors (GIST), 5 malignant peripheral nerve sheath tumors (MPNST), 12 synovial sarcomas, 28 MFH (10 myxoid and 18 pleomorphic), and 10 leiomyosarcomas (7 conventional and 3 pleomorphic) (Supplementary Fig. 1 and Supplementary Table 1).

The frozen samples were crushed to powder with a CryoPress (Microtech Nichion, Chiba, Japan) under cooling with liquid nitrogen. The frozen powder was then homogenized with urea lysis buffer (6 M urea, 2 M thiourea, 3% CHAPS, 1% triton X-100). After centrifugation at 15 000 rpm for 30 min, the supernatant was used as the source of cellular proteins for protein expression studies.

2.2 Protein expression profiling

Protein expression profiles were obtained by 2-D difference gel electrophoresis (2-D-DIGE). The internal control consisted of a mixture of all the protein samples used in this study. The internal control sample and the individual sample were labeled with the CyDye DIGE Fluor saturation dyes Cy3 and Cy5 (GE Healthcare Amersham Biosciences), respectively. The Cy3-labeled control sample and the Cy5-labeled individual sample were mixed and coseparated by 2-D PAGE. After electrophoresis, the gels were scanned at appropriate wavelengths for Cy3 and Cy5 to generate the images of the reference sample and the individual sample, respectively. We ran triplicate gels for each sample, and in total 240 gels were run and 480 images were created for the 80 samples. The ratio between Cy5 intensity and Cy3 intensity was calculated for all spots in each gel with DeCyder software (GE Healthcare Amersham Biosciences) to obtain the standardized spot intensities. As the Cy3 image represents the internal standard sample, this standardization procedure eliminates gel-to-gel differences. The standardized spot intensities were logarithmically transformed, averaged for triplicate gels and analyzed with the data-mining package Impressionist (GeneData, Basel, Switzerland).

To assess the reproducibility of the proteomic data in our analyses, we compared the protein profiles obtained from three independent separations of sample L-10 (Fig. 1A, Supplementary Table 1). Scatter plot analysis revealed that the standardized intensity of more than 99% of the spots was scattered within a 2.0-fold difference. We used the averaged spot intensity from the triplicate gels for further data analysis.

2.3 Data analysis

We identified the proteins that were informative for classification by using a support vector machine algorithm and a leave-one-out crossvalidation [16, 17]. First, we selected the spots that appeared in more than 75% of Cy3 images. Second, the multiclass problem was solved by a series of seven one-*versus*-all comparisons (*e.g.*, "clear cell sarcoma" *vs.* "not clear cell sarcoma") and the spots with expression levels significantly different between two groups of different tumor types were selected on the basis of the Wilcoxon method. The pairwise similarity of expression profiles was examined for the spots between all samples to exclude irrelevant samples. Third, we developed classifiers by using the support vector

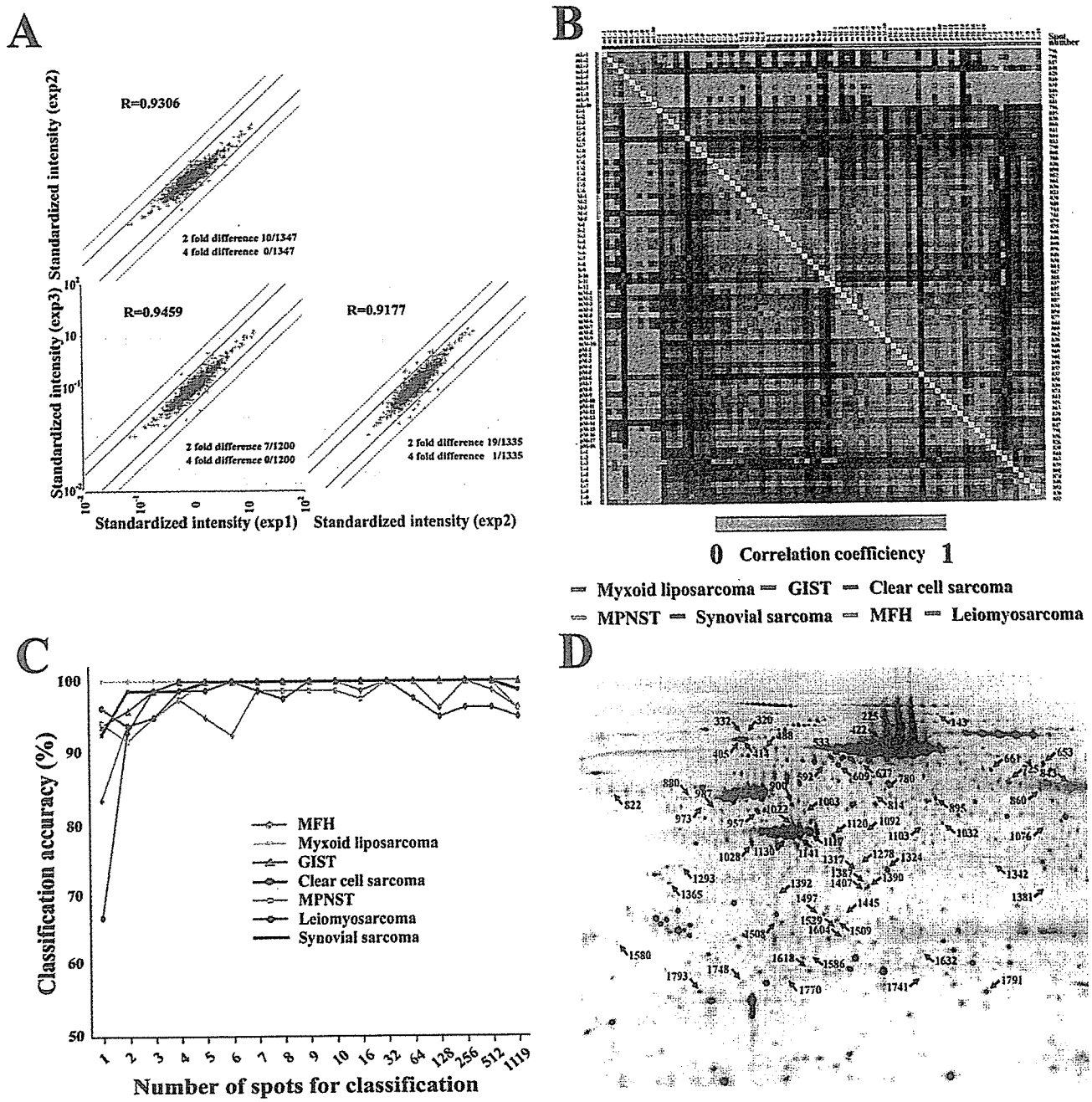

Figure 1. Spot selection for histological classification. (A) Evaluation of reproducibility of 2-D-DIGE by scattergram. (B) Correlation matrix of the 80 sarcomas on the basis of the expression profiles of the selected spots. The sarcomas were ordered by histological class and color-coded. The patient ID corresponds to that in Supplementary Table 1. The number of spots examined is listed on the right (Supplementary Fig. 3A). (C) Mean leave-one-out crossvalidation accuracy was plotted as a function of the number of spots used by each classifier. (D) Localization of the selected 67 spots on the image of the 2-D PAGE. Protein identification is summarized in Supplementary Table 2.

machine and the accuracy of the classifiers was evaluated by a leave-one-out crossvalidation. The process was repeated for each sample, and the cumulative crossvalidation error rate was calculated. Fourth, we ranked all protein spots according to their relative contribution to the classification on the basis of support vector machine weight. By calculating the cumulative error rate while eliminating proteins in the order of increasing rank, we examined the relationship between the number of proteins and classification accuracy. Fifth, the classification performance of a candidate classifier was evaluated by multivariate analysis including principal component analysis and hierarchical clustering.

2.4 Protein identification by MS and Western blotting

Proteins corresponding to the spots of interest were identified by MS. Cy5-labeled proteins separated by 2-D PAGE were recovered in gel plugs and digested with modified trypsin (Promega, Madison, WI, USA). The trypsin digests were subjected to LC coupled with MS/MS on a machine equipped with a nanoelectrospray ion source. A search of the mass of the peptide ion peaks against the Swiss-Prot database was performed with MASCOT software. Protein identification and differential expression were confirmed by Western blotting using specific antibodies against tropomyosin isoforms.

2.5 Role of the funding source

The sponsors of the study had no role in study design, data collection, data analysis, data interpretation, or writing of the report.

3 Results

Protein expression profiling was performed for the 80 soft-tissue sarcomas by 2-D-DIGE. We selected protein spots that appeared in at least 75% of the 240 images of the Cy3-labeled internal control sample and that showed different spot intensities between one histological subgroup and the other tumors (Wilcoxon test, $p < 0.01$). Although potentially resulting in the loss of information, this trimming process decreased the possibility that the classifier would be significantly influenced by irrelevant expression data. We observed the pairwise similarity of the protein expression profiles of the 80 samples. A correlation matrix showed that the myxoid liposarcoma samples had a distinct protein expression profile that differed from that of the rest of the tumor samples, which shared a similar overall protein expression profile (Fig. 1B and Supplementary Fig. 3A). However, hierarchical clustering using all protein spots did not result in the classification of soft-tissue sarcomas according to their histology (Supplementary Fig. 2). At this stage we tried to omit irrelevant samples that could hinder the proper classification. However, as we could not identify obviously anomalous samples (Fig. 1B and Supplementary Fig. 3A), we used all 80 samples in the subsequent study. We selected protein sets of which the expression was associated with the existing histological classification by using a support vector machine. The accuracy, plotted as a function of spot number, was constant until the number of spots decreased to less than five, showing that accurate classification did not require all protein spots (Fig. 1C). We decided to study the top ten ranked protein spots for each classification and evaluate their classification performance. As three spots overlapped among the 70 spots, 67 spots were selected (Fig. 1D and Supplementary Fig. 4). The results of classification, shown as the distance of a sample from the hyper-plane, demonstrated that all samples except one were classified correctly with the trained support vector machine (Supplementary Fig. 5). Mass spectrometric study identified the proteins corresponding to these 67 spots, revealing that the 67 spots were products of 67 different genes (Supplementary Table 2). The pairwise correlation matrix of the 80 samples showed that sarcomas in the same histological group had a common expression profile of the 67 proteins (Fig. 2A and Supplementary Fig. 3B). To evaluate the classification performance of the 67 protein spots, we performed principal component analysis of the 80 samples with the 67 spots (Fig. 2B). Liposarcoma and leiomyosarcoma showed a distinct protein expression profile and the other tumors were also grouped with those of the same histological background. In contrast, the profiles of three pleomorphic leiomyosarcoma samples (L-1, L-5, and L-7) were separated from that of conventional leiomyosarcoma, and close to that of MFH.

To examine correlations among tumors with different histological backgrounds, we performed hierarchical clustering. Hierarchical clustering with the 67 spots yielded two clusters of tumors (Fig. 2C and Supplementary Fig. 6). All samples of leiomyosarcoma and MFH fell within Cluster 1. Cluster 2 contained two major groups – one consisting of with myxoid liposarcomas, and the other of clear cell sarcomas, synovial sarcomas, MPSNTs, and GISTs. In Cluster 1, pleomorphic leiomyosarcoma (L-1, L-5, and L-7) and conventional leiomyosarcoma (L-2, 3, 4, 6, 8, 9, and 10) were divided into two branches; all three pleomorphic leimyosarcomas were separated from the conventional leiomyosarcomas and associated with the MFH samples, consistent with the results of principal component analysis (Fig. 2B). We identified the proteins responsible for leiomyosarcoma subtypes. Supervised classification of pleomorphic and conventional leiomyosarcomas identified ten proteins as the most different features of the leiomyosarcoma subclasses (the process of spot selection is demonstrated in Supplementary Fig. 7 and the results of protein identification are summarized in Supplementary Table 2). Hierarchical classification using the selected ten spots divided leiomyosarcoma samples into pleomorphic and conventional types, validating the results of the support vector machine classification (Fig. 3A). Use of specific antibodies confirmed the differential expression of tropomyosin isoforms between these two groups of leiomyosarcoma, also showing that relative protein amounts measured by 2-D-DIGE and Western blotting were highly correlated (Fig. 4 and Supplementary Fig. 8). Pleomorphic leiomyosarcoma and MFH shared the similar expression pattern of tropomyosine isoforms (Supplementary Fig. 9).

Histological grading has been correlated with patient outcome [18]. Using protein expression profiles of 10 leiomyosarcomas and 28 MFHs, we investigated the proteins that could distinguish between these tumors of grades I/II and those of grade III. Supervised classification identified a set of five proteins by which the crossvalidation error rate was minimal for these two tumor groups (the process of spot

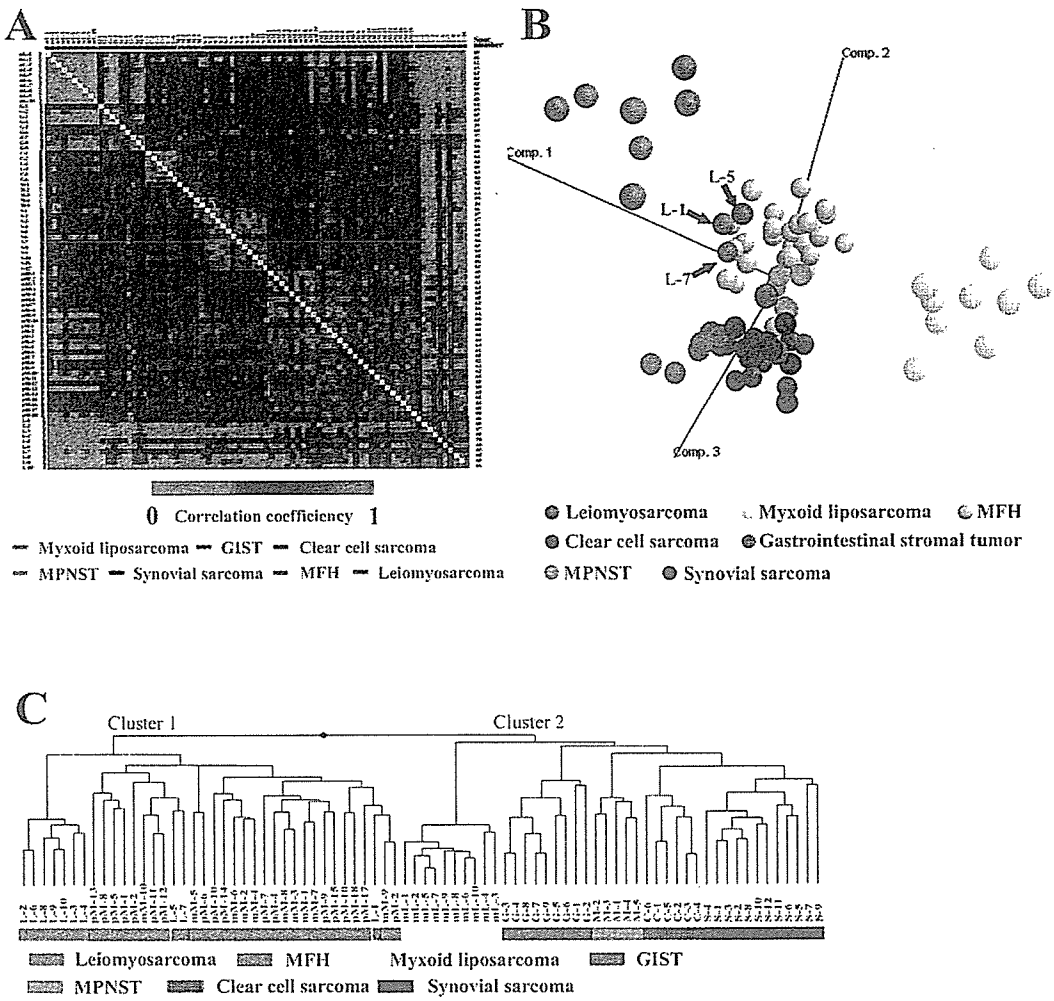

Figure 2. Classification of soft-tissue sarcoma by the selected 67 spots. (A) Correlation matrix using the protein expression profiles. (B) Principal component analysis of the 80 soft-tissue tumors on the basis of the expression profiles of the 67 proteins. Arrows indicated three pleomorphic leiomyosarcomas (L-1, L-5, and L-7). (C) Hierarchical classification on the basis of a distance tree constructed from the 67 proteins. The name of the 67 proteins used for the classification and their expression level were described in Supplemental Figure 6.

selection is demonstrated in Supplementary Fig. 10 and the results of protein identification are summarized in Supplementary Table 2). Hierarchical clustering using these five proteins divided 38 tumor samples into two groups (Fig. 3B). Nine of 11 samples in Cluster 1 showed histological grades I/II, and 25 of 27 samples in Cluster 2 were categorized in grade III. Although tumors with grades I/II and those with grade III did not show significantly different patient survivals in our study (p = 0.0857, Fig. 5A), the patients in Cluster 1 and those in Cluster 2 showed distinct survival rates (p = 0.0296, Fig. 5B). Hierarchical clustering subdivided Cluster 2 into two groups: Clusters 2a and 2b (Fig. 3B). The difference in patient survival between Clusters 1 and 2a was only suggestive (p = 0.0811). In contrast, patients in Cluster 2b had a significantly worse survival relative to those in Clusters 1 and 2a (p = 0.0028 and 0.0271, respectively; Fig. 5C).

4 Discussion

Identification of molecular signatures corresponding to histological subtypes is an essential step toward understanding of the molecular basis of tumor development. We generated protein expression profiles of 80 soft-tissue tumors from seven histological backgrounds and identified protein clusters unique to the histology. We identified a set of 67 proteins that showed distinctive expression patterns in the subclasses of soft-tissue sarcomas. Hierarchical clustering demonstrated that leiomyosarcomas and MFHs shared similar expression pattern of these 67 proteins (Fig. 2C and Supplementary Fig. 6). DNA microarray study also showed that these two tumors had similar gene expression profile [4]. The recent studies with comparative genomic hybridization (CGH) revealed that leiomyosarcoma and MFH had similar CGH imbalance profiles [19]. These observations suggested

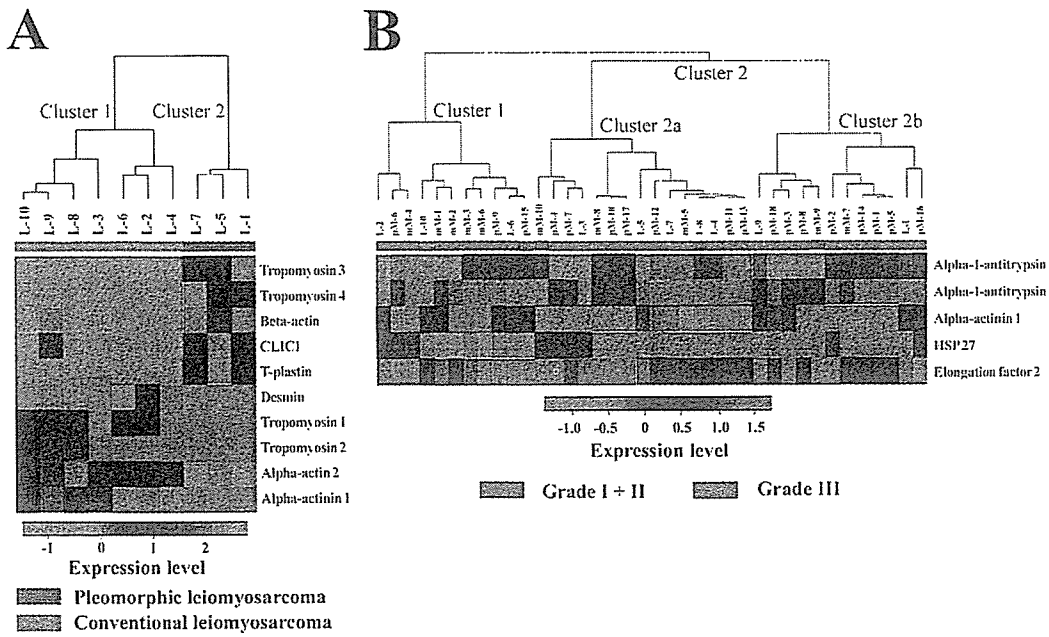

Figure 3. (A) Classification of leiomyosarcomas from expression of ten selected proteins. (B) Histological grading of leiomyosarcoma and MFH from expression of five proteins.

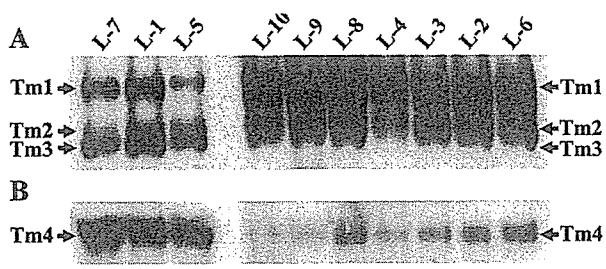

Figure 4. Western blotting for tropomyosin isoforms with specific antibodies. Specific antibodies against tropomyosin 1, 2, and 3 (A) and against tropomyosin 4 (B) were reacted with the leiomyosarcoma samples blotted on the membrane. As the antibody for tropomyosin 1, 2, and 3 did not distinguish these three isoforms, identification was achieved by the electrophoretic migration of the bands according to a previous report [32].

that these tumor types might correspond to different differentiation states of a single tumor. In our study, pleomorphic leiomyosarcoma was distinct from conventional leiomyosarcoma and close to MFH in terms of protein expression (Fig. 2B and C and Supplementary Fig. 6), probably reflecting different biological behavior and proliferating activities [20]. We noted that GIST, MPSNTs, clear cell sarcomas, and synovial sarcomas had similar protein expression profile (Fig. 2C and Supplementary Fig. 6). The similarity of these four tumor types is consistent with the biological association and similar gene expression of these tumor types. For example, clear cell sarcoma is known as melanoma of the soft parts, which was proposed to arise from a progenitor neural crest cell with the potential for melanocytic differentiation and melanin synthesis [21]. Gene expression study showed that synovial sarcoma and MPNST shared differential expression of several genes characteristic of neural crest-derived cells [5]. GIST may be derived not from the muscle cells in the intestinal tract but from neuronal cells with pacemaker activity in the bowel wall [22]. Gene expression profiling suggested the close association of GIST with synovial sarcoma [4]. These observations lead to the idea that the status of genome, transcriptome, and proteome may be reflected by the histological appearance of tumors and the identification of most critical genes or proteins for the classification will provide the diagnostic molecular markers for soft-tissue sarcoma.

We demonstrated that the expression levels of five protein spots including HSP27 were associated with histological grading and patient survival in leiomyosarcoma and MFH. HSP27 expression is associated with a favorable prognosis in MFH, correlating with overall survival and metastasis-free survival [23]. The prognostic value of HSP27 has also been suggested in many other types of cancer, including ovarian carcinoma [24], brain tumor [25], and gastric cancer [26]. Expression of the other proteins has also been correlated with the malignant characteristics of tumors. Up-regulated production of alpha-1-antitrypsin mRNA has been reported in pancreatic cancer [27] and liver cancer [28]. Modulation of alpha-actinin levels affected cell motility and conferred tumorigenicity on 3T3 cells [29]. In our study, multiple isoforms of alpha-actinin 1 were identified as informative proteins for histological classification, leiomyosarcoma subclassification, and histological grading (Supplementary Table 2). These isoforms were distinguished as different

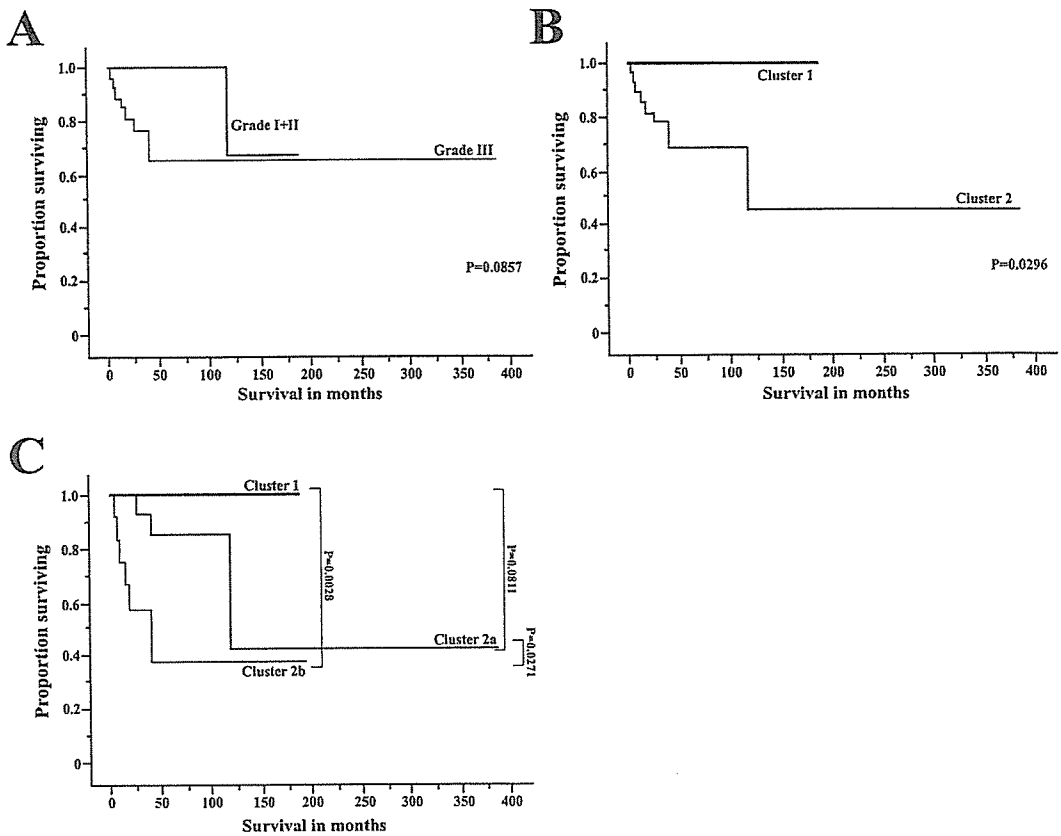

Figure 5. Kaplan–Meier survival curves for the groups with histological grading I/II and III (A) and for the groups of Clusters 1 and 2 in Fig. 3B. (B) Kaplan–Meier survival curves were also plotted for the groups of Clusters 1, 2a and 2b (Fig. 3B). *p* values were obtained by the log-rank test.

spots on the 2-D image and probably arise from PTMs. These isoforms may have different functional properties that contribute to the histological appearance and biological behavior of the tumors. Proteins associated with survival can be considered as a candidate for prognostic tumor marker, by which we can delineate a high-risk group that may benefit from adjuvant therapy and exclude low-risk patients in whom additional therapies are unlikely to exhibit clinical benefit.

We did not identify several known correlations between certain genes and tissue types, including between KIT and GIST [4], between SSX and synovial sarcoma [30], and between melanoma antigens and clear cell sarcoma [31]. This discrepancy is probably a result of the limited sensitivity of 2-D DIGE. As 2-D DIGE detects proteins nonspecifically according to amount, the expression levels of these oncoproteins may be below the LOD. Extensive efforts are being directed toward uncovering a greater fraction of the proteome by improving the sensitivity of current proteomic technologies, and such efforts will further benefit our understanding of the biology of soft-tissue sarcomas.

Genome-wide protein expression profiling will lead to the identification of important proteins and to novel molecular classifications. Our experiments revealed the proteins associated with histological classification and grading. The diagnostic and prognostic performance of the identified proteins will be validated in larger numbers of patients. As these proteins could also be involved in the development of soft-tissue sarcomas, study of their expression might contribute to novel therapeutic strategies.

This work was supported by a grant from the Ministry of Health, Labor, and Welfare and by the Program for Promotion of Fundamental Studies in Health Sciences in the National Institute of Biomedical Innovation of Japan.

The corresponding author had full access to all the data in the study and had final responsibility for the decision to submit for publication. The corresponding author declared that there is no conflict of interest.

5 References

[1] Borden, E. C., Baker, L. H., Bell, R. S., Bramwell, V. *et al.*, *Clin. Cancer Res.* 2003, *9*, 1941–1956.

[2] Hasegawa, T., Yamamoto, S., Nojima, T., Hirose, T. *et al.*, *Hum. Pathol.* 2002, *33*, 111–115.

[3] Fletcher, J. A., *Cytogenetic Analysis of Soft Tissue Tumors*, 4th Edn., St. Louis, Mosby 2001.

[4] Nielsen, T. O., West, R. B., Linn, S. C., Alter, O. *et al.*, *Lancet* 2002, *359*, 1301–1307.

[5] Nagayama, S., Katagiri, T., Tsunoda, T., Hosaka, T. *et al.*, *Cancer Res.* 2002, *62*, 5859–5866.

[6] Segal, N. H., Pavlidis, P., Antonescu, C. R., Maki, R. G. *et al.*, *Am. J. Pathol.* 2003, *163*, 691–700.

[7] Chen, G., Gharib, T. G., Huang, C. C., Taylor, J. M. *et al.*, *Mol. Cell. Proteomics* 2002, *1*, 304–313.

[8] Gygi, S. P., Rochon, Y., Franza, B. R., Aebersold, R., *Mol. Cell. Biol.* 1999, *19*, 1720–1730.

[9] Varambally, S., Yu, J., Laxman, B., Rhodes, D. R. *et al.*, *Cancer Cell* 2005, *8*, 393–406.

[10] Chen, G., Gharib, T. G., Wang, H., Huang, C. C. *et al.*, *Proc. Natl. Acad. Sci. USA* 2003, *100*, 13537–13542.

[11] Yanagisawa, K., Shyr, Y., Xu, B. J., Massion, P. P. *et al.*, *Lancet* 2003, *362*, 433–439.

[12] Alaiya, A. A., Franzen, B., Hagman, A., Dysvik, B. *et al.*, *Int. J. Cancer* 2002, *98*, 895–899.

[13] Dwek, M. V., Alaiya, A. A., *Br. J. Cancer* 2003, *89*, 305–307.

[14] Reyzer, M. L., Caldwell, R. L., Dugger, T. C., Forbes, J. T. *et al.*, *Cancer Res.* 2004, *64*, 9093–9100.

[15] Cui, J. W., Wang, J., He, K., Jin, B. F. *et al.*, *Clin. Cancer Res.* 2004, *10*, 6887–6896.

[16] Brown, M. P., Grundy, W. N., Lin, D., Cristianini, N. *et al.*, *Proc. Natl. Acad. Sci. USA* 2000, *97*, 262–267.

[17] Ramaswamy, S., Tamayo, P., Rifkin, R., Mukherjee, S. *et al.*, *Proc. Natl. Acad. Sci. USA* 2001, *98*, 15149–15154.

[18] Fletcher, C. D. M., *Soft Tissue Tumours: Epidemiology, Clinical Features, Histological Typing and Grading*, IARC Press, Lyon 2002.

[19] Derre, J., Lagace, R., Nicolas, A., Mairal, A. *et al.*, *Lab. Invest.* 2001, *81*, 211–215.

[20] Oda, Y., Miyajima, K., Kawaguchi, K., Tamiya, S. *et al.*, *Am. J. Surg. Pathol.* 2001, *25*, 1030–1038.

[21] Chung, E. B., Enzinger, F. M., *Am. J. Surg. Pathol.* 1983, *7*, 405–413.

[22] Kindblom, L. G., Remotti, H. E., Aldenborg, F., Meis-Kindblom, J. M., *Am. J. Pathol.* 1998, *152*, 1259–1269.

[23] Tetu, B., Lacasse, B., Bouchard, H. L., Lagace, R. *et al.*, *Cancer Res.* 1992, *52*, 2325–2328.

[24] Geisler, J. P., Tammela, J. E., Manahan, K. J., Geisler, H. E. *et al.*, *Eur. J. Gynaecol. Oncol.* 2004, *25*, 165–168.

[25] Assimakopoulou, M., Sotiropoulou-Bonikou, G., Maraziotis, T., Varakis, I., *Anticancer Res.* 1997, *17*, 2677–2682.

[26] Takeno, S., Noguchi, T., Kikuchi, R., Sato, T. *et al.*, *Ann. Surg. Oncol.* 2001, *8*, 215–221.

[27] Trachte, A. L., Suthers, S. E., Lerner, M. R., Hanas, J. S. *et al.*, *Am. J. Surg.* 2002, *184*, 642–647; discussion 647–648.

[28] Anderson, S. P., Cattley, R. C., Corton, J. C., *Mol. Carcinog.* 1999, *26*, 226–238.

[29] Gluck, U., Ben-Ze'ev, A., *J. Cell Sci.* 1994, *107*, 1773–1782.

[30] dos Santos, N. R., de Bruijn, D. R., van Kessel, A. G., *Genes Chromosomes Cancer* 2001, *30*, 1–14.

[31] Granter, S. R., Weilbaecher, K. N., Quigley, C., Fletcher, C. D., *Mod. Pathol.* 2001, *14*, 6–9.

[32] Pawlak, G., McGarvey, T. W., Nguyen, T. B., Tomaszewski, J. E. *et al.*, *Int. J. Cancer* 2004, *110*, 368–373.

Proteomics 2006, *6*, 0000–0000 DOI 10.1002/pmic.200500883

RESEARCH ARTICLE

Plasma proteomics of lung cancer by a linkage of multi-dimensional liquid chromatography and two-dimensional difference gel electrophoresis

Tetsuya Okano[1, 4], Tadashi Kondo[1], Tatsuhiko Kakisaka[1], Kiyonaga Fujii[1], Masayo Yamada[1], Harubumi Kato[2, 3], Toshihide Nishimura[2], Akihiko Gemma[4], Shoji Kudoh[4] and Setsuo Hirohashi[1]

[1] Proteome Bioinformatics Project, National Cancer Center Research Institute, Tokyo, Japan
[2] Clinical Proteome Center, Tokyo Medical University, Tokyo, Japan
[3] Department of Surgery, Tokyo Medical University, Tokyo, Japan
[4] Fourth Department of Internal Medicine, Nippon Medical School, Tokyo, Japan

To investigate aberrant plasma proteins in lung cancer, we compared the proteomic profiles of serum from five lung cancer patients and from four healthy volunteers. Immuno-affinity chromatography was used to deplete highly abundant plasma proteins, and the resulting plasma samples were separated into eight fractions by anion-exchange chromatography. Quantitative protein profiles of the fractionated samples were generated by two-dimensional difference gel electrophoresis, in which the experimental samples and the internal control samples were labeled with different dyes and co-separated by two-dimensional polyacrylamide gel electrophoresis. This approach succeeded in resolving 3890 protein spots. For 364 of the protein spots, the expression level in lung cancer was more than twofold different from that in the healthy volunteers. These differences were statistically significant (Student's *t*-test, *p*-value less than 0.05). Mass spectrometric protein identification revealed that the 364 protein spots corresponded to 58 gene products, including the classical plasma proteins and the tissue-leakage proteins catalase, clusterin, ficolin, gelsolin, lumican, tetranectin, triosephosphate isomerase and vitronectin. The combination of multi-dimensional liquid chromatography and two-dimensional difference gel electrophoresis provides a valuable tool for serum proteomics in lung cancer.

Received: December 6, 2005
Revised: February 19, 2006
Accepted: March 12, 2006

Keywords:
Lung cancer / Multi-dimensional liquid chromatography / Two-dimensional difference gel electrophoresis

1 Introduction

Lung cancer is a leading cause of cancer death in Japan, claiming 55 000 lives annually, and is a major health problem in many countries. The prognosis of patients with lung cancer is generally poor, with an overall 5-year survival rate for patients receiving treatment of only 14%. In contrast, overall 5-year survival for patients diagnosed with stage I adenocarcinoma approaches 63% [1]. As non-small-cell lung cancer accounts for almost 80% of lung cancers, of which 40% are adenocarcinoma, a substantial number of patients with lung cancer have the potential to be cured successfully by early treatment. However, the majority of lung tumors have reached locally advanced stage III (33%) or metastatic stage IV (41%) by the time of diagnosis [2]. Therefore, early diagnosis of lung cancer is necessary to improve patient survival. Plasma is a preferred specimen for the early diagnosis of lung cancer because samples are easily available by non-

Correspondence: Professor Tadashi Kondo, Proteome Bioinformatics Project, National Cancer Center Research Institute, 5-1-1 Tsukiji, Chuo-ku, Tokyo 104-0045, Japan
E-mail: takondo@gan2.res.ncc.go.jp
Fax: +81-3-3547-5298

invasive methods. However, the currently available plasma tumor markers such as CEA, NSE, TPA, chromogranin, CA125, CA19–9, Cyfra 21–1, and ProGRP have limited sensitivity and specificity for early diagnosis [3], and novel plasma markers are required.

Multi-dimensional separation techniques based on the combination of LC and gel electrophoresis have been applied for plasma proteomics [4]. Typically, LC with immuno-affinity, size-exclusion, ion-exchange and RP columns is used to fraction the proteins, which are then subjected to high-resolution 2-D-PAGE for quantitative expression studies. Sample fractionation prior to 2-D-PAGE can separate gene products present in low copy numbers from highly abundant proteins, increasing the number of observable proteins. Indeed, less abundant proteins, including tissue-leakage proteins and regulatory proteins, have been identified in plasma by the combination of LC and 2-D-PAGE [4]. As the results of 2-D-PAGE can be quantified and stored in a database, 2-D-PAGE is a powerful tool for biomarker development. However, the intrinsic limitations of 2-D-PAGE resulting from gel-to-gel variations can hinder accurate comparisons of protein expression levels. To cancel such experimental differences, 2-D-DIGE has been developed [5–7]. In 2-D-DIGE, the experimental samples and an internal control sample are labeled with different fluorescent dyes, mixed together and co-separated in identical gels. The fluorescent dyes are designed so that the electrophoretic migration of proteins labeled with the different dyes is almost identical. Therefore, the intensity of the spots of the experimental sample can be normalized to the intensity of the corresponding spots of the internal control sample in the same gel. In 2-D-DIGE the amounts of proteins are measured as fluorescence signals, thus the dynamic range is wider than with conventional silver staining and spot detection can be achieved by simple laser scanning in a high-throughput manner. 2-D-DIGE has been used to characterize the proteome of plasma from patients with disease [8]. Recently, novel highly sensitive fluorescent dyes, CyDye DIGE Fluor saturation dyes (GE Healthcare Amersham Biosciences, Uppsala, Sweden), referred to here as 'saturation dye', have been developed [9]. The high sensitivity of saturation dye has enabled proteomic studies of primary cultured human hepatocytes [10] and laser-microdissected tumor tissues [11–14], where only limited amounts of proteins were available.

In this study, we used the combination of multi-dimensional chromatography and 2-D-DIGE with saturation dye to conduct a proteomic comparison of serum from patients with lung cancer and from healthy volunteers. The high sensitivity of saturation dye generated 3890 protein spots from only 30 μL of plasma. We identified 364 spots as aberrantly regulated plasma proteins in lung cancer. MS revealed that these spots corresponded to 58 gene products. The identified proteins included previously uncharacterized tissue-leakage proteins in addition to acute phase plasma proteins. These results demonstrate the utility of multi-dimensional LC and 2-D-DIGE for plasma proteomics in cancer.

2 Materials and methods

2.1 Serum samples

Blood samples by venipuncture and informed consent were obtained from five patients with lung cancer and four healthy volunteers at Nippon Medical School. Clinical information for the donors of serum proteins is summarized in Table 1. A 10-mL blood sample was obtained with a VENOJECT II (10 mL; TERUMO, Tokyo, Japan) and allowed to clot for 2 h at 4°C. The clotted material was removed by centrifugation at 3000 rpm for 10 min. The supernatant sera obtained from the blood samples were recovered and stored at −80°C until use.

Table 1. Patients' characteristics

	Histology [29]	Gender	Age (years)	Stage [30]
1.	Adenocarcinoma	Male	48	T2N2M0 IIIA
2.	Adenocarcinoma	Male	62	T4N2M0 IIIB
3.	Squamous cell carcinoma	Female	75	T4N3M1 IV
4.	Squamous cell carcinoma	Male	76	T4N1M1 IV
5.	Small cell carcinoma	Male	40	T2N2M0 IIIA
Four healthy volunteers		4 Males	29~38	

2.2 Immuno-affinity and anion-exchange chromatography

Serum proteins were separated by immuno-affinity and ion-exchange chromatography with the AKTA Explore system (GE Healthcare Amersham Biosciences). The immuno-affinity column (4.6 × 100 mm; Agilent Technologies) contained anti-albumin, anti-transferrin, anti-haptoglobin, anti-alpha-1-anti-trypsin, anti-IgA and anti-IgG resins. A serum sample (30 μL) was diluted with 120 μL of a neutral buffer (buffer A; Agilent Technologies), and filtered with a spin filter (pore size 0.22 μm; Agilent Technologies) by centrifugation at 16 000 × g for 1 min prior to use. The filtered sample was applied to the immuno-affinity column at a flow rate of 0.5 mL/min for 10 min. The flow-through fraction was recovered and the proteins retained in the column were eluted with a low-pH urea buffer (buffer B; Agilent Technologies) at a flow rate of 1.0 mL/min for 10 min. The column was recycled for further use by washing with buffer A at a flow rate of 1.0 mL/min for 12 min. The flow-through fractions were concentrated to 500 μL in a Spin Concentrator, 5K MWCO (4 mL capacity, Agilent Technologies).

The concentrated sample was diluted with 4.5 mL of 25 mM Tris-HCl, pH 9.0, and applied to a Resource Q column (1.0 mL resin, 6.4 mm id × 30 mm; GE Healthcare

Amersham Biosciences) at a flow rate of 4.0 mL/min. The separations were performed with a step-wise gradient of NaCl as follows: 0 mM for 12.5 min, 100, 150, 200, 250, 300, 350, and1000 mM for 2.5 min each. All elution buffers contained 25 mM Tris-HCl, pH 9.0. The anion-exchange column was then recycled for further use by thorough washing with 25 mM Tris-HCl, pH 9.0, containing 2 M NaCl. In the interval between the elution steps, the pump system was washed with 10 mL of the next elution buffer. Protein peaks were monitored at 280 nm. The eluted proteins were concentrated with Amicon Ultra PL-10 (a molecular mass cut-off 10 kDa) in an Amicon Ultra-15 filter unit (Amicon Bredford, MA).

2.3 2-D DIGE

The fractionated proteins were precipitated by addition of four volumes of acetone at −20°C for 20 min. After centrifugation at 13 000 rpm for 10 min, the supernatant was discarded and the pellet was air-dried for 10 min. The dried pellet was dissolved in 50 μL of lysis buffer containing 6 M urea, 2 M thiourea, 3% CHAPS, 1% Triton X-100 and 40 mM Tris (pH 8.0). The protein concentration was measured with a Protein Assay Kit (Bio-Rad Laboratories, Hercules, CA). The fluorescence labeling was performed as described previously with some modifications [10]. In brief, samples (50 μg of protein) were reduced by incubation with 2 μM Tris-(2-carboxethyl)phosphine hydrochloride (TCEP; Sigma, St. Louis, MO) at 37°C for 60 min. The protein samples were fluorescence labeled by incubation with 40 nM of saturation Cy3 or Cy5 dye (GE Healthcare Amersham Biosciences) at 37°C for another 30 min. For 2-D-PAGE, the labeling reaction was terminated by addition of an equal volume of the lysis buffer containing 130 mM DTT and 2.0% Pharmalyte (Amersham Biosciences). In the fraction eluted with 1000 mM NaCl, the amount of protein was so small that its concentration could not be measured. Therefore, all the protein in these fractions was labeled and used for the subsequent studies. As the trains of spots in the vertical dimension were not observed on 2-D images, we concluded that the proteins were saturatedly labeled with fluorescent dyes.

The 2-D-PAGE was carried out as described previously in our reports [11]. In brief, the first dimension separation was carried out with Immobiline Drystrips (24 cm, pH 3–10; GE Healthcare Amersham Biosciences). Each strip was rehydrated for 12 h at 30 V with 420 μL of protein sample, and IEF was performed in an IPGphor unit (GE Healthcare Amersham Bioscience). After electrophoresis, the strips were equilibrated in equilibration buffer (6 M urea, 2% SDS, 50 mM Tris HCl, pH 8.8, 30% glycerol w/v) for 20 min. The second dimension separation was performed on homemade 9–15% gradient polyacrylamide gels with an EttanDalt II system (GE Healthcare Amersham Biosciences) at a constant wattage of 17 W at 20°C for 17 h. The image was acquired by scanning the gels with a laser scanner (2D MasterImager; GE Healthcare Amersham Biosciences). Spot detection, quantification and image matching were performed with DeCyder software (GE Healthcare Amersham Biosciences). One portion of the labeled proteins was separated by SDS-PAGE using 10% polyacrylamide gel to monitor the contents of the fractions. Gel electrophoresis was performed in the dark.

2.4 Protein identification by MS

In-gel digestion was performed for protein spots excised by an automated spot collector (SpotPicker; GE Healthcare Amersham Biosciences), according to our previous report [10]. Then, the gel pieces were extensively washed with ammonium bicarbonate. The protein in the dried gel plug was digested overnight at 37°C with sequencing-grade modified trypsin (Promega, Madison, WI). The tryptic digests were recovered by incubation with 50% ACN/0.1% TFA, and the isolated peptides were concentrated under nitrogen gas and subjected to LC-MS/MS. The MS study was carried out as described previously [15]. In brief, the LC-MS/MS system comprised a Paradigm MS4 dual solvent delivery system (Michrom BioSciences, Auburn, CA, USA) for HPLC, an HTS PAL auto sampler with two 10-port injector valves (CTC Analytics, Zwingen, Switzerland), and a Finnigan LTQ linear ITMS (Thermo Electron, San Jose, CA, USA) equipped with NSI sources (AMR, Tokyo, Japan). A database search against Swiss-Prot was performed with MASCOT software. When multiple proteins were identified in a single spot, the proteins with the highest numbers of peptides were considered as those corresponding to the spots. When multiple protein candidates were listed with an equal number of the identified peptides, the proteins with a higher MASCOT score were selected.

2.5 Western blotting

Protein samples were separated by SDS-PAGE and transferred onto NC membranes. Differential expression of plasma proteins was examined by specific antibodies against leucine-rich alpha 2 glycoprotein (x1000 dilution; Abnova, Taiwan), inter-alpha-trypsin inhibitor heavy chain H4 (x1000 dilution; Santa Cruz Biotechnology, Santa Cruz, CA), plasma retinol binding protein (x50 dilution; Biomeda), haptoglobin (x2000 dilution; Sigma Aldrich, St. Louis, MO, USA), complement component C4 (x200 dilution; Antibody Shop, Gentofte, Denmark), complement component C3 (x200 dilution; Antibody Shop), and prothrombin (x100 dilution; BD Transduction laboratories). The anti-prothrombin antibody could recognize both thrombin and prothrombin. A second antibody against goat IgG (Santa Cruz Biotechnology) was used for inter-alpha-trypsin inhibitor heavy chain H4 at a dilution of 1:2000. A second antibody against mouse IgG (GE Healthcare Amersham Biosciences) was used for leucine-rich alpha 2 glycoprotein, plasma retinol-binding protein, haptoglobin, complement component C4, complement component C3 and prothrombin at a dilution of 1:1000. Immune complexes were detected with an enhanced

chemiluminescence system (GE Healthcare Amersham Biosciences) and monitored with an LAS-1000 (Fuji Film, Tokyo, Japan).

3 Results

3.1 Evaluation of the fractionation process

In the first dimension chromatography, we used a recently developed immuno-affinity column to deplete the most abundant plasma proteins, including albumin, immunoglobulin, transferrin, anti-trypsin, and haptoglobin. This immuno-affinity column has been employed for plasma proteomics to enrich the less abundant plasma proteins [4, 16–18]. Whole serum was separated into two fractions: the flow-through fraction containing low abundance serum proteins and the bound fraction containing the abundant proteins listed above (Fig. 1A). Proteins in the flow-through fraction were subjected to anion-exchange chromatography (Fig. 1B). To ensure reproducibility of protein overlap between neighboring fractions, we employed step-wise separation instead of gradient separation. In addition, we washed the column with the elution buffer at the end of each fraction step to reduce the carry-over of elution buffer between the steps. To evaluate the reproducibility of the fractionation process, the 250-mM NaCl fraction of three independently prepared protein samples was separated by RP chromatography (Fig. 1C). The three chromatograms showed that the fractionation process was highly reproducible.

To examine the effects of fractionation, the protein samples were labeled with fluorescent dyes and separated by SDS-PAGE (Fig. 2). The major bands in the unfractionated serum proteins, as indicated by arrows (lane 1), were observed in the bound fraction of the immuno-affinity column (lane 3). Proteins in the flow-through fraction of the immuno-affinity column generated a higher number of bands (lane 2). The other portion of this fraction was further separated by anion-exchange chromatography, labeled with fluorescent dyes and subjected to SDS-PAGE (lanes 4–11). The fractions from anion-exchange chromatography showed distinct protein migration patterns (lanes 4–11) compared with the unfractionated serum (lane 1) and the flow-through fraction of the immuno-affinity column (lane 2). Anion-exchange chromatography combined with immuno-affinity chromatography reduced the complexity and dynamic range of the protein content and separated the less abundant proteins from the neighboring highly abundant proteins, resulting in an increase in the number of observable proteins.

We conducted 2-D-PAGE to separate further the fractionated proteins. The 2-D-PAGE allows detection of post-translational differences, observed as a shift in p*I* that are difficult to recognize by SDS-PAGE. To validate the effects of fractionation on the number of observable proteins, we labeled a whole-serum sample and a fractionated protein

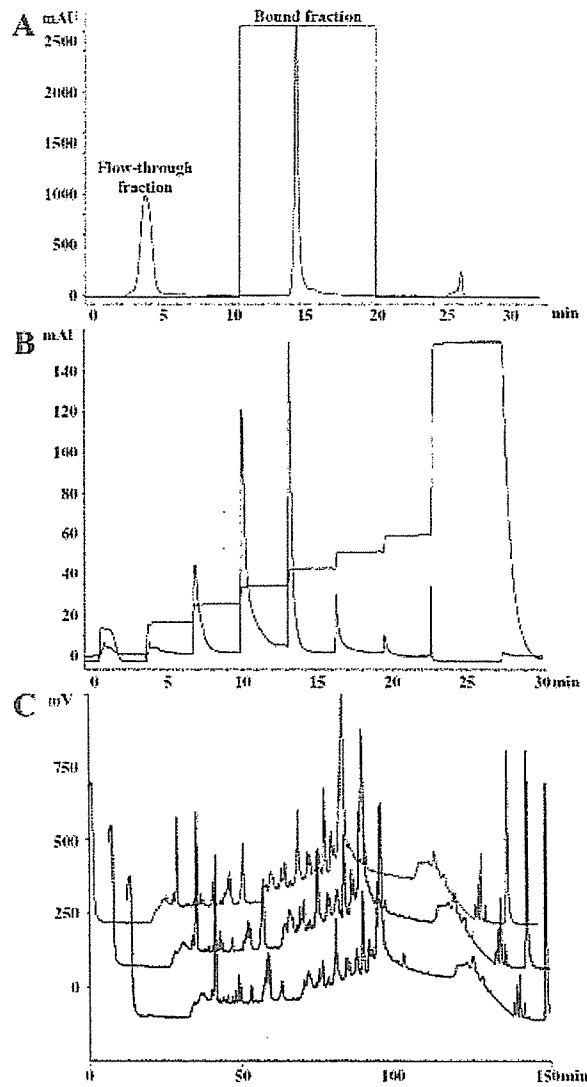

Figure 1. Process of multi-dimensional chromatography separation. (A) The immuno-affinity column separated plasma proteins into two fractions: flow-through and bound fraction. The column was recycled by washing after elution of the bound proteins. (B) The flow-through fraction from the immuno-affinity column was subjected to anion-exchange chromatography and separated into eight fractions by elution with a step-wise gradient of NaCl. (C) Three independent samples of the 250 mM NaCl fraction were prepared and separated by RP chromatography to examine the reproducibility of the immuno-affinity and anion-exchange procedures.

sample with Cy3 and Cy5, respectively, mixed them together and co-separated them by 2-D-PAGE. Figure 3 shows the two-color images of whole-serum (red) and fractionated proteins (green). It is apparent that most of the protein spots that bound to, and were recovered from the immuno-affinity column, matched the spots with high intensity in whole

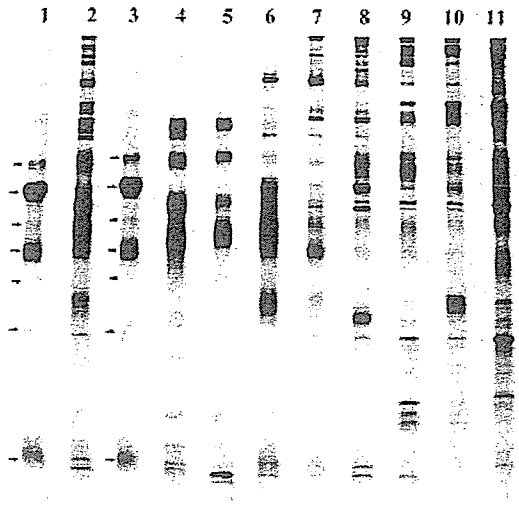

Figure 2. Separation of whole and fractionated plasma samples by SDS-PAGE. Lane 1, whole serum sample; lane 2, flow-through fraction from the immuno-affinity column; lane 3, bound fraction from the immuno-affinity column; lanes 4–11, the fractions eluted by 0, 100, 150, 200, 250, 300, 350 and 1000 mM NaCl from the anion-exchange column.

serum (panel A). In contrast, immuno-depletion of these proteins resulted in a distinct 2-D image; most of the protein spots in the flow-through fraction of the immuno-affinity column were not observed in the 2-D image of whole serum (panel B). These results are consistent with previous reports [17, 19]. We also separated the Cy5-labeled fractions from anion-exchange chromatography by 2-D-PAGE (panels C–J). Visual comparison of the location and intensity of spots through the series of 2-D images can be achieved easily by using the Cy3 image of whole serum as a common internal standard. It is clear that the number of spots was increased by fractionation with anion-exchange chromatography. However, it is unclear how many proteins repeatedly appeared as different spots in the gels.

3.2 Comparison of serum from patients with lung cancer and healthy volunteers

We compared serum proteins in patients with lung cancer and healthy volunteers (Table 1). We prepared a mixture of the paired protein samples to make an internal standard and labeled it with Cy3. The individual samples were labeled with Cy5 and mixed with the Cy3-labeled internal standard sample. The mixture of labeled protein samples was separated by 2-D-PAGE. Figure 4 shows a representative gel image of Cy5-labeled proteins. The number of spots observed is described in the lower right corner of the 2-D image panel. The number of spots in the mixture of unfractionated serum of patients with lung cancer and of healthy volunteers was 124, and fractionation increased the total number of spots to 3766. The arrows indicate the 364 spots whose expression in lung cancer differed significantly by more than twofold from that in the healthy volunteers (Student's *t*-test, *p*-value less than 0.05). MS identified the proteins from the spots. We observed multiple proteins from single spots in several cases. These observations were consistent with the previous report [20]. Tentatively, the proteins with the highest number of peptides were considered to be the proteins corresponding to the spots, although this is not always the case. Based on this criterion, we concluded that MS study of these 364 spots resulted in the identification of 58 distinct gene products. The results of protein identification are summarized in Suppl. Table 1.

We found that certain proteins appeared on the 2-D images as multiple protein spots with aberrantly controlled expression in lung cancer. In addition, different protein spots translated from the same gene showed different regulation, so that isoforms of a particular plasma protein could be up- or down-regulated in lung cancer. Figure 5 summarizes these observations. Among 58 proteins identified, 18 were detected as a single spot. These were alpha-1-acid glycoprotein, apolipoprotein D, apolipoprotein M, carbonic anhydrase II, catalase, ceruloplasmin, complement C5, corticosteroid-binding globulin, Ig alpha-1 chain C region, Ig gamma-1 chain C region, Ig kappa chain V-III region SIE, inter-alpha-trypsin inhibitor heavy chains H1, H2 and H4, kininogen, tetranectin, triosephosphate isomerase, and vitronectin. Spots for 28 proteins showed consistent up- or down-regulation (Fig. 5A) and the spots for 12 proteins showed inconsistent regulation (Fig. 5B). For example, the intensity of all 67 haptoglobulin spots was increased in lung cancer, whereas for the 38 spots of complement component C3 the intensity of 20 spots was up-regulated and that of 18 spots was down-regulated in lung cancer. Thus, isoform-specific regulation may exist for these proteins.

We then used specific antibodies to validate the differential expression of the plasma proteins whose isoforms showed consistent aberrations in lung cancer (Fig. 6), because clinical application of our results would require differential expression to be monitored by methods more convenient than the combination of multi-dimensional LC and 2-D-DIGE. We examined individual samples by SDS-PAGE followed by Western blotting with specific antibodies. The higher intensity of the lower bands of leucine-rich alpha-2-glycoprotein in lung cancer was consistent with the results of multi-dimensional chromatography followed by 2-D-PAGE (Fig. 6A). The intensity of the upper bands of leucine-rich alpha-2-glycoprotein did not differ between the two groups and the spots corresponding to these bands were not recognized as those showing aberrant intensity in lung cancer (Fig. 6A). The higher intensity of haptoglobulin bands was also consistent with the results of 2-D-PAGE (Fig. 6D). However, the intensities of the bands of inter-alpha-trypsin inhibitor heavy chain H4 (Fig. 6B) and plasma retinol binding protein (Fig. 6C) were also higher in lung cancer, and these results were inconsistent with those from multi-

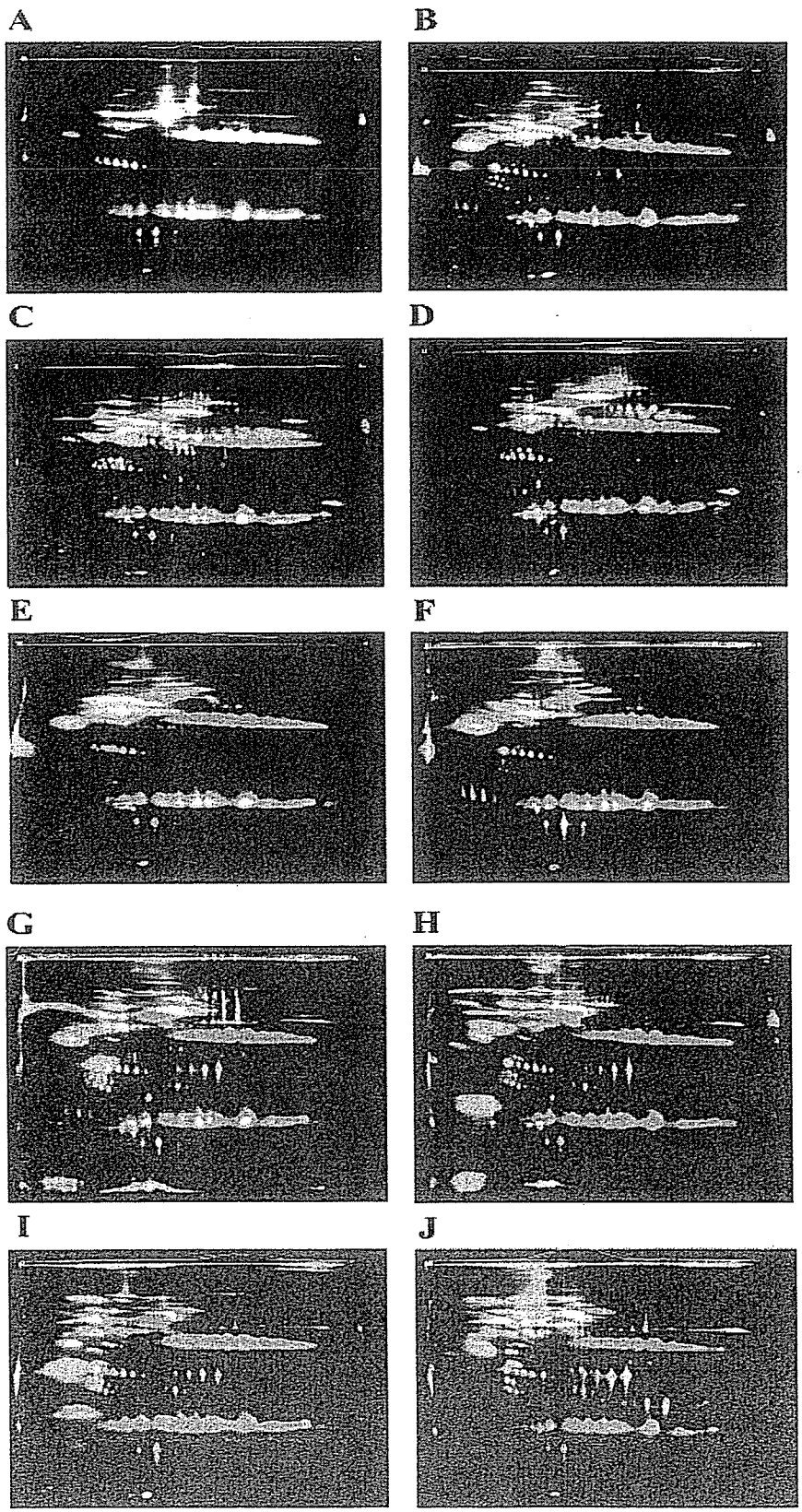

Figure 3. 2-D-PAGE of plasma proteins. Whole serum and fractionated proteins were labeled with Cy3 (red) and Cy5 (green), respectively. The labeled protein samples were mixed together and co-separated by 2-D-PAGE. The fractionated proteins showed distinguishable protein profiles, suggesting the efficient enrichment of low abundance proteins by fractionation. The sources of the protein samples are as follows: (A) bound fraction from the immuno-affinity column; (B) flow-through fraction from the immuno-affinity column; (C–J) 2-D images of the fractions eluted with 0, 100, 150, 200, 250, 300, 350 and 1000 mM NaCl from the anion-exchange column.

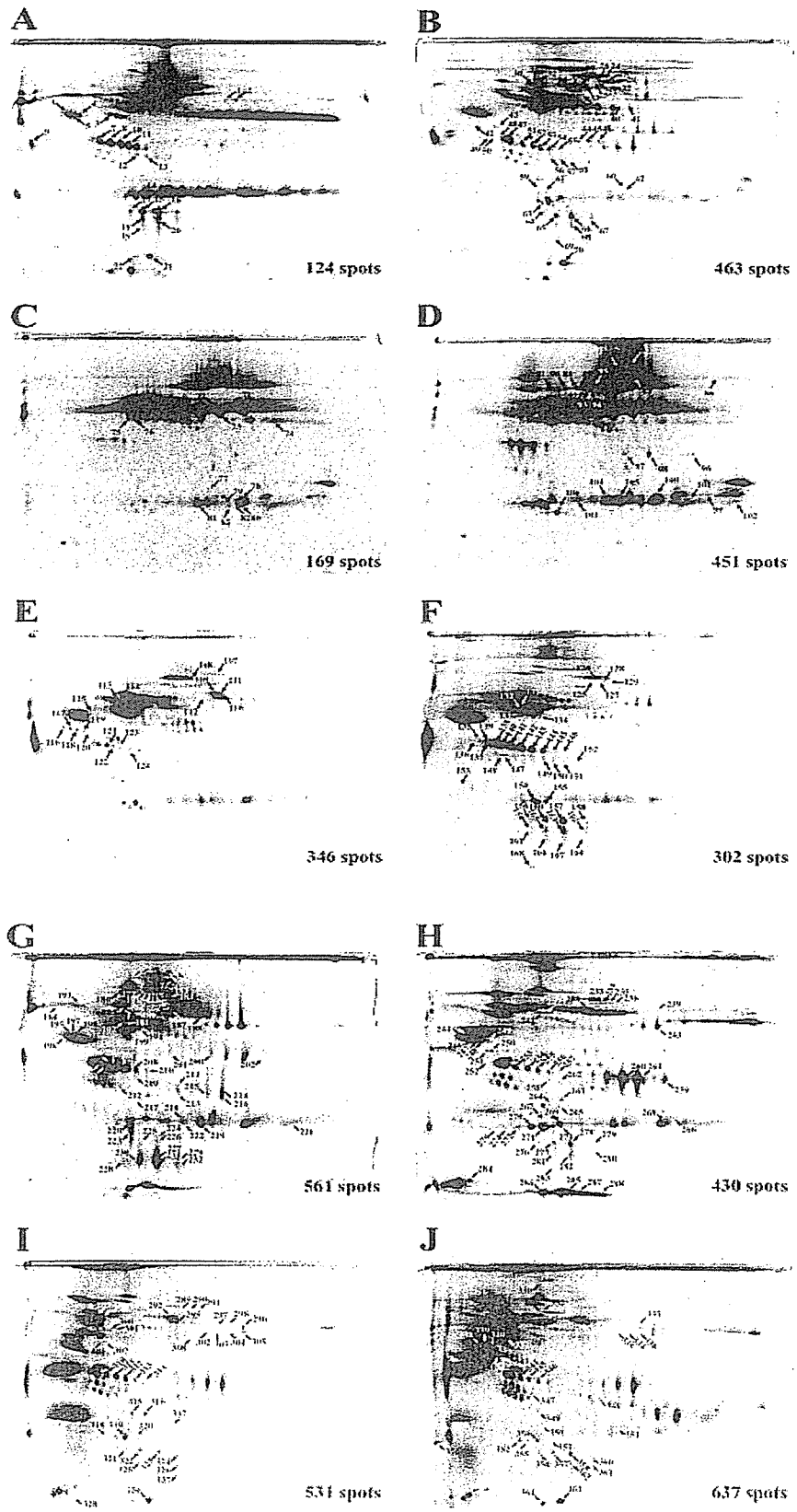

Figure 4. Localization of spots on the 2-D map of Cy5-labeled proteins. The arrows indicate the spots showing aberrant expression in lung cancer. The spot numbers correspond to those in Suppl. Table 1. The sources of the protein samples are as follows: (A) unfractionated serum; (B) flow-through fraction from the immuno-affinity column; (C–J) 2-D images of the fractions eluted with 0, 100, 150, 200, 250, 300, 350 and 1000 mM NaCl from the anion-exchange column.

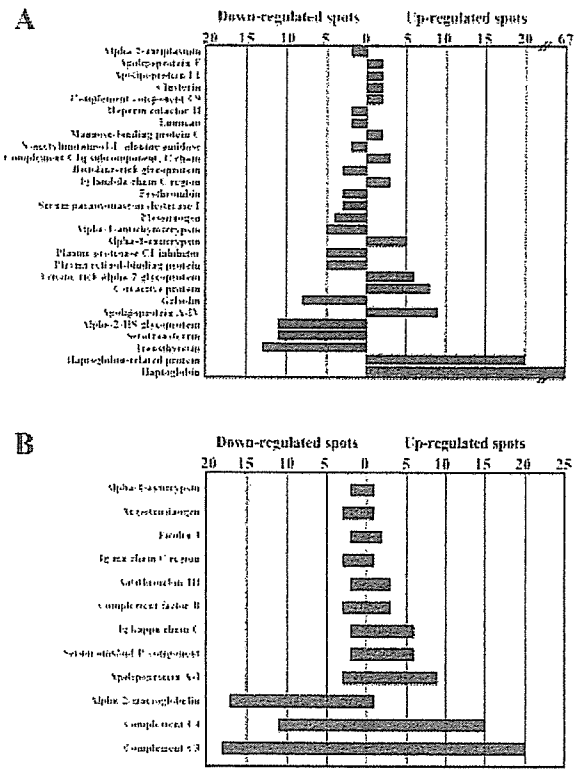

Figure 5. Analysis of spots showing aberrant expression levels in lung cancer. (A) Proteins for which the corresponding spots showed consistent differences in lung cancer; (B) proteins for which the corresponding spots showed inconsistent differences in lung cancer. X-axis representss the number of protein spots identified as those showing a significantly aberrant expression level in lung cancer. The 18 proteins identified as single spots were described in Section 3.

dimensional chromatography followed by 2-D-PAGE. We also studied the expression of complement component C4, whose isoforms showed differential expression. Complement component C4 consists of three subunits with molecular masses of 97, 75 and 33 kDa. The antibody we used visualized the 97-kDa band (Fig. 6E). On 2-D gel images, the expression level of the C4 spots of molecular mass approximately 97 kDa was increased in lung cancer. Western blotting identified increased expression of complement component C3, with a molecular mass of 45 kDa, though the C3 spots with this molecular weight showed both up- and down-regulated intensity in lung cancer (Fig. 6F). These results may indicate that complement component C3 is up-regulated as a whole in lung cancer and that 2-D-DIGE detects minor isoforms that are regulated in a different way from the major (abundant) isoforms. Western blotting also revealed an increased expression of prothrombin, with a molecular mass of 50 kDa, in lung cancer, and this result was inconsistent with the data obtained by 2-D-DIGE (Fig. 6G). Western blotting demonstrated increased expression of pro-

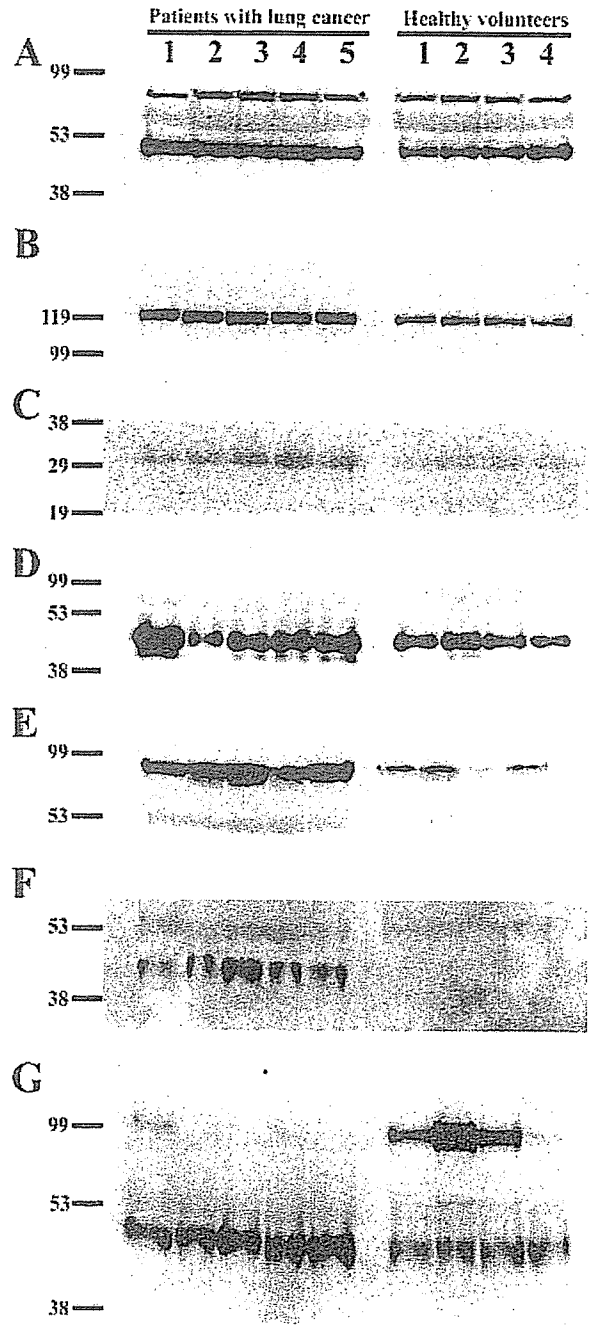

Figure 6. Validation of the differential expression of plasma proteins between individuals. Western blotting using (A) anti-leucine-rich alpha 2 glycoprotein, (B) anti-inter-alpha-trypsin inhibitor heavy chain H4, (C) anti-plasma retinol-binding protein, (D) anti-haptoglobin, (E) anti-complement component C4, (F) anti-complement component C3, and (G) anti-prothrombin antibody.

thrombin with a molecular mass of 99 kDa in three of four healthy volunteers (Fig. 6G), and this increase was not observed by 2-D-DIGE (Fig. 4).

4 Discussion

We applied a highly sensitive fluorescent dye-labeling technique to multi-dimensional chromatography followed by 2-D-PAGE for lung cancer plasma proteomics. In this study, the proteins were separated in three dimensions according to their net charge, p*I* and molecular weight. Pieper *et al.* [4] reported a similar approach to the plasma proteome. In their report, human serum samples were separated into 74 fractions by immuno-affinity, anion-exchange, and size-exclusion chromatography. The fractionated samples were then subjected to 2-D-PAGE, yielding approximately 3700 protein spots. They identified by MS 325 proteins corresponding to about 1800 spots. In our study, we observed 3890 spots and identified 58 proteins corresponding to 364 spots. As we focused on proteins with aberrant expression in lung cancer and did not perform global protein identification, it is difficult to compare the performance of these two methods, although most proteins we identified were also identified in [4]. However, our use of highly sensitive fluorescent dyes has several advantages over the method used in this report, as exemplified by the following four points. First, Pieper *et al.* [4] used 20 mL of serum as a starting material, whereas we needed only 30 μL of plasma to obtain a similar number of spots. The different amount of plasma protein required for the analysis was probably a result of the sensitivity of the spot detection method, as Pieper *et al.* visualized the proteins by staining with CBB G-250, which is less sensitive than saturation dye. The amount of plasma sample available may be limited, and a method requiring less sample may be more suitable for clinical proteomics. Alternatively, our protocol may have the potential to visualize even less abundant plasma proteins by increasing the sample volume. Secondly, gel staining with CBB G-250 is time-consuming (more than 3 days in the study of Pieper *et al.*), whereas spot detection of fluorescence-labeled proteins can be completed within 30–60 min by a laser scanner. This feature is especially advantageous because several 2-D gels are required for each of the fractionated samples. Thirdly, the fluorescent dye-labeling method may allow more quantitative and reproducible protein expression profiling by running an internal control sample and generating multiplex images. Forthly, the linear dynamic range of protein expression level measured as fluorescent intensity in 2-D-DIGE is wider than that in conventional 2-D-PAGE based on a colorimetric method such as CBB G-250.

Wang *et al.* [17] reported the utility of the fluorescent dye-labeling technique in the linkage of IEF, LC and SDS-PAGE for the study of intact plasma proteins. They identified plasma proteins associated with acute graft-versus-host disease. In their protocol, the highly abundant plasma proteins were depleted with an immuno-affinity column. Low abundance proteins were then labeled with fluorescent dyes, mixed, and subjected to IEF and RP chromatography. Finally, the fractionated proteins were separated by SDS-PAGE and detected by laser scanning. To label the proteins, they used minimal dye, which labels lysine residues [9]. Although minimal dye is less sensitive than saturation dye, minimal dye is advantageous when three samples are to be compared because Cy2 is available in addition to Cy3 and Cy5 [18].

The results of this study are consistent with previous reports of aberrant expression of plasma proteins in lung cancer. Alpha-1-acid glycoprotein in plasma has been shown to be highly sensitive and specific for the detection of lung cancer [21], and its levels are correlated with treatment effects and prognosis in patients with non-small-cell lung cancer treated with docetaxel [22]. The utility of retinol-binding protein for the diagnosis of lung cancer has also been described [23]. We also found aberrant expression of tissue-leakage plasma proteins whose expression in tumor cells is correlated with lung cancer. For example, we found that the expression level of clusterin was increased in lung cancer. Clusterin is a component of membrane-coated vesicles and has a protective function in cells. Previous studies have revealed that inhibition of clusterin expression enhances the effects of paclitaxel or gemcitabine in delaying the growth of A549 tumors [24]. We also found decreased expression of gelsolin in lung cancer. Down-regulation of gelsolin in tumor cells was correlated with poor survival of patients with non-small-cell lung cancer [25]. Although the pathophysiological significance of these tissue-leakage proteins is largely obscure, their clinical application as candidate tumor markers should be considered.

In this study, we did not identify proteins showing very low abundance such as growth factors, suggesting that further development of the current protocol is required for a comprehensive understanding of the lung cancer proteome. Block *et al.* [26] reported that they observed low abundance tissue-leakage proteins as spots on 2-D images when they fractionated plasma samples with a lectin-affinity column. Thus, additional variations of multi-dimensional separation including multiple specific immuno-affinity columns will facilitate the study of lower abundance plasma proteins.

The proteins retained in the immuno-affinity column were not limited to the six target plasma proteins (Fig. 2). Albumin is known to interact with a variety of proteins [27], and as the proteins were separated as intact forms in our study, depletion of albumin may cause the removal of unexpected proteins. We also identified alpha-1-anti-trypsin, haptoglobin, and transferrin in the fractionated samples as aberrantly regulated plasma proteins in lung cancer, even though our procedure was designed to deplete these proteins at the initial step of fractionation by use of the immuno-affinity column. Together, these observations suggest that the immuno-depletion procedure requires

